ORGANOMETALLICS

Communication

pubs.acs.org/Organometallics

# Rhodium Complexes of a New Structurally Adaptive PNN-Pincer Type Ligand

Sarath Wanniarachchi, Jeewantha S. Hewage, Sergey V. Lindeman, and James R. Gardinier*

Department of Chemistry, Marquette University, Milwaukee, Wisconsin 53201-1881, United States

Supporting Information

**ABSTRACT:** A new PNN-pincer type ligand with pyrazolyl and diphenylphosphine flanking donors on a diarylamido anchor has been prepared. Its bis(*tert*-butyl isocyanide)rhodium(I) complex exhibits hemilabile behavior in solution, and its solid-state structure verified the elusive $\kappa^2P,N$ coordination mode for this type of ligand. Reactions between (PNN)Rh(CN$^t$Bu)$_2$ and iodomethane afford both *fac*- and *cis,mer*-[(PNN)Rh(CN$^t$Bu)$_2$(Me)](I), which further showcases the structural versatility of the ligand.

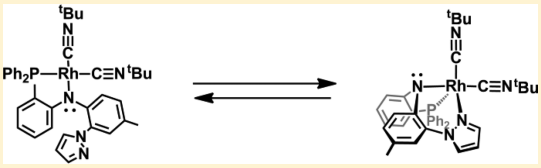


Over the past few decades, there has been intense interest in metal complexes of multidentate "hemilabile" ligands where one ligating arm readily dissociates or is forcibly displaced by an incoming nucleophile.[1] The identification and study of such hemilabile ligands has been important both for the development of new catalytic reactions and for the discovery of new materials for sensing applications.[2] A majority of hemilabile ligands are bidentate[3] with both "hard" and "soft" Lewis donors. Other ligands such as tris(pyrazolyl)borate, tris(pyrazolyl)methanes, and related "scorpionates", which typically bind metals in a facial terdentate manner with six-membered chelate rings, have also been shown to be hemilabile with certain metals.[4] There has been a growing interest in complexes of hemilabile "pincer" ligands (typically anionic terdentate species that bind metals with five-membered rings), because certain examples have been found to mediate remarkable chemical transformations.[5] The van der Vlugt group recently reported on the hemilabile/"flexidentate" character of bis(isopropyl isonitrile)rhodium(I) complexes of two PNN-pincer (**A** and **C**, Chart 1) and one pincer-type (**B**, Chart 1) ligand.[6] The authors provided compelling spectroscopic evidence that various (PNN)Rh(CNR)$_2$ complexes contained four-coordinate rhodium with $\kappa^2P,N$ ligands, but in no case was a complex structurally authenticated. Instead, computational studies were used to support the assertion that one ligand arm was dissociated, since "no minimum (corresponding to a five-coordinate species) could be located on either respective potential energy surface". Given our experience with diarylamido-anchored ligands with six-membered chelate rings similar to complex **B**, we were keenly aware that, although less common than the *mer* coordination mode, the *fac* coordination mode is sometimes observed.[7] Such a possibility casts doubt on the structural nature of the reported (PNN)Rh(CNR)$_2$ complexes. Thus, we set out to exploit the crystallinity of pyrazolyl-containing ligand systems to structurally verify the elusive $\kappa^2P,N$ coordination mode of the (PNN)Rh(CNR)$_2$ complexes. In this paper, we document useful coupling reactions to obtain a new pyrazolyl-containing ligand with a PNN donor set. We also describe the syntheses of various rhodium(I) complexes and the hemilability of one complex. The variability in metal coordinating behavior of the new pincer-type ligand is also illustrated through examination of [(PNN)Rh(Me)(CN$^t$Bu)$_2$](I).

**Chart 1. Rhodium(I) Complexes of Hemilabile PNN-Pincer Ligands Reported by the van der Vlugt Group[6]**

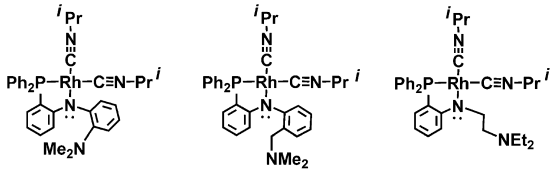


The synthetic route to the new ligand and its carbonylrhodium(I) complex is outlined in Scheme 1. A CuI-catalyzed amination reaction between 2-pyrazolyl-4-toluidine (H(pzAn$^{Me}$))[8] and diiodobenzene affords 2-iodo-*N*-(4-methyl-2-(1*H*-pyrazol-1-yl)phenyl)benzenamine, (H(N$^{IPh}$- pzAn$^{Me}$)), a precursor (top right of Scheme 1) that is used in the final step of the ligand construction. A high-yielding Pd$^0$-catalyzed coupling reaction between H(N$^{IPh}$-pzAn$^{Me}$) and HPPh$_2$ provides the desired ligand with a PNN donor set (the crystal structure of H(PNN) and further synthetic discussion are found in the Supporting Information). The reaction between Rh(CO)$_2$(acac) and H(PNN) in acetone afforded a high yield of (PNN)Rh(CO) (**1**). Complex **1** is air stable in the solid state as well as in solution, and no special precautions were required for its handling. Although all attempts to obtain crystals of **1** suitable for X-ray diffraction have been stymied by its propensity to form microcrystalline needles, the NMR spectral

**Received:** February 24, 2013
**Published:** May 3, 2013

**Scheme 1.** [a]

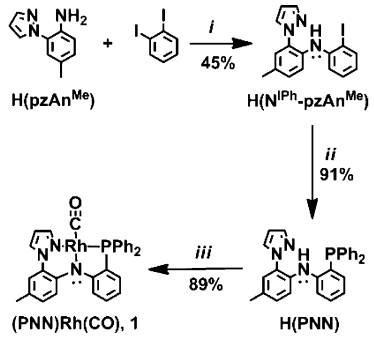


[a]Key: (i) cat. CuI, 1.2 $Cs_2CO_3$, *p*-dioxane, Δ 16 h; (ii) 1.2 $HPPh_2$, 0.5 mol % $Pd_2(dba)_3$, 1 mol % Xantphos, 1.2 $NEt_3$, *p*-dioxane, Δ, 15 h; (iii) $Rh(CO)_2(acac)$, acetone, Δ, 15 min.

data of **1** are in accord with the structural formulation depicted in Scheme 1. The C−O stretching frequency for **1**, $\nu_{CO}$ 1957 $cm^{-1}$, is comparable to $\nu_{CO}$ 1960 $cm^{-1}$ reported for the related PNP derivative of Mayer and Kaska with a diarylamido anchor and two $PPh_2$ flankers.[9] Another related complex, (NNN)Rh-(CO) (**2**; NNN has two pyrazolyl flanking donors attached to the same diarylamido backbone as in **1**), has a C−O stretching frequency of $\nu_{CO}$ 1954 $cm^{-1}$,[10] which indicates only a slight increase in back-bonding in comparison to **1**. These comparable results corroborate our previous findings that the *para* aryl substituents (rather than flanking donors) dictate the electronic properties of the metal complexes of diarylamido-anchored pincer ligands. The $^{13}C$ NMR spectrum of **1** shows a doublet of doublets signal at $\delta_C$ 193 ppm ($^1J_{Rh-C}$ = 67 Hz and $^2J_{P-C}$ = 18 Hz) for the rhodium-bound carbonyl; that for **2** showed a doublet resonance at $\delta_C$ 193 ppm ($^1J_{Rh-C}$ = 71 Hz). The similarity of chemical shift and coupling constant between **1** and **2** suggests that **1** has a square-planar coordination geometry about rhodium with *trans*-disposed amido and carbonyl groups like that in the structurally characterized **2**. The $^{31}P$ NMR spectrum of **1** shows a doublet resonance at $\delta_P$ 61 ppm ($^1J_{P-Rh}$ = 167 Hz), which is shifted downfield from the singlet resonance at $\delta_P$ = −20 ppm for H(PNN) and the doublet resonance at $\delta_P$ 41.8 ppm ($^1J_{P-Rh}$ = 135.1 Hz) reported for Mayer and Kaska's PNP derivative.[9]

Complex **1** reacts with excess (4 equiv or more) of $CN^tBu$ to give analytically pure $(PNN)Rh(CN^tBu)_2$ (**3**). As reported for other similar complexes, complex **3** is air sensitive both in the solid state and in solution. Thus, **3** needs to be stored and handled under an inert atmosphere. Single crystals of **3** suitable for X-ray diffraction were grown by extracting the initial product mixture of **1** and excess $CN^tBu$ with pentane and allowing the pentane-soluble portion to stand under nitrogen for several hours. The structure of **3** shown in Figure 1 verifies the $\kappa^2P,N$ coordination mode of the ligand. The rhodium is in a square-planar geometry, where the sum of angles about the metal is 360°. The isocyanide ligand *trans* to the amido exhibits a shorter Rh−C bond (1.888(2) Å) and a marginally longer unsaturated C−N bond (1.156(8) Å) in comparison with that *trans* to the phosphine arm (Rh−C, 1.983(2) Å; C−N, 1.141(9) Å). The Rh−C bond distances are the ranges found for other charge-neutral rhodium(I) organoisocyanide complexes.[12−16] The Rh−N and Rh−P bonds in **3** are similarly unremarkable.

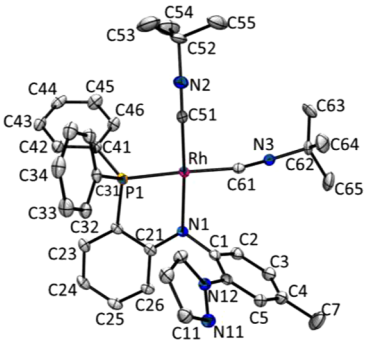


**Figure 1.** Structure of $(PNN)Rh(CN^tBu)_2$ in **3**·0.2(pentane), with hydrogen atoms removed for clarity. Thermal ellipsoids are shown at the 50% probability level. Selected bond distances (Å): Rh1−P1, 2.2521(5); Rh1−N1, 2.0728(14); Rh1−C51, 1.8884(18); Rh1−C61, 1.9825(18); C51−N2, 1.156(8); N2−C52, 1.472(8); C61−N3, 1.141(9); N3−C62, 1.457(9); Selected bond angles (deg): P1−Rh1−N1, 82.42(4); P1−Rh1−C51, 93.70(6); C51−Rh1−C61, 88.40(7); N1−Rh1−C61, 95.48(6); N1−Rh1−C51, 176.10(7); P1−Rh1−C61, 177.63(5); C51−N2−C52, 177.3(8); C61−N3−C62, 173.3(17).

Dynamic behavior for **3** in solution is evident from an examination of variable-temperature NMR spectral data. The resonances for various nuclei show different temperature-dependent line broadening and changes in chemical shifts depending on the type of resonance. Figure 2 shows an overlay

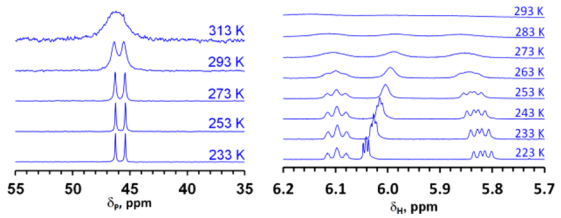


**Figure 2.** Overlays of the $^{31}P$ NMR spectra (left) and representative portion of the $^1H$ NMR spectra (right) of **3** in acetone-$d_6$ obtained at various temperatures.

of $^{31}P$ NMR spectra and a representative portion of the $^1H$ NMR spectra for **3** in acetone-$d_6$ at various temperatures (more complete spectra can be found in the Supporting Information). At 223 K, the $^{31}P$ NMR spectrum consists of a doublet at 45.8 ppm with $J_{RhP}$ = 138.5 Hz. When the temperature is raised above 243 K, the doublet resonance shifts slightly downfield and becomes broader until coupling can no longer be detected above 303 K. As can be seen in Figure 2 and Figures S4 and S5 (Supporting Information), similar behavior occurs for resonances in the $^1H$ NMR spectra, but with notable differences. The resonances for the pyrazolyl, tolyl, and one of the *tert*-butyl group (upfield signal) hydrogens exhibit the greatest line broadening and changes in chemical shifts, followed by resonances for the $PC_6H_4N$ group. The resonances for the hydrogens of the $(C_6H_5)_2P$ group and the other $^tBu$ group exhibit negligible changes with temperature. The rate constant of the dynamic process can be extracted by measuring $W_{1/2}$, the line broadening in excess of the natural line width, according to the relation $k = \pi W_{1/2}$. As detailed in the Supporting Information, Eyring analyses (Figure S6) of the temperature dependence of the line broadening/rate constant derived from the $^{31}P$ NMR resonance and the $^1H$ NMR resonances for pyrazolyl, tolyl, and upfield $^tBu$ hydrogens afforded the


dx.doi.org/10.1021/om400151e | *Organometallics* 2013, 32, 2885−2888

following activation parameters: $\Delta G^{\ddagger}$ = 14.3 (±0.1) kcal/mol, $\Delta H^{\ddagger}$ = 9 (±2) kcal/mol, and $\Delta S^{\ddagger}$ = −19(±5) cal/(K mol). The negative value for activation entropy suggests a highly organized transition state. On the basis of experimental observations and theoretical calculations (OP86/Def2-SV-(P))[11] that show a five-coordinate conformer is only 5.1 kcal higher in energy than a four-coordinate structure (Figure S10, Supporting Information), we attribute the dynamic process to be a result of reversible coordination of the hemilabile pyrazolyl arm ($k_{298}$ = 229 $s^{-1}$), as in Scheme 2. Such a proposition

**Scheme 2. Plausible Process Responsible for Temperature-Dependent NMR Line Broadening in the Spectra of 3**

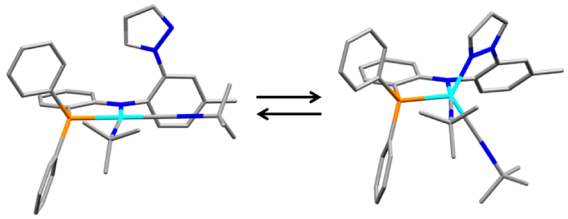

rationalizes the observed trends in the disparate broadening of resonances and chemical shift changes in the NMR spectra. Also, the possible presence of both four- and five-coordinate isomers of **3** at room temperature provides an explanation for the greater than expected number of CN stretches observed in the IR spectra. Theoretical calculations indicate that two CN stretches are expected at 2164 and 2101 $cm^{-1}$ (in a 0.99 intensity ratio) for four-coordinate **3** and at 2147 and 2075 $cm^{-1}$ (in an intensity ratio of 1.05) for five-coordinate **3**. The experimentally observed CN stretching frequencies for **3** in benzene occur at 2156, 2102, and 2065 $cm^{-1}$ with relative intensities of 1.9:1:1.2. Thus, the relatively high intensity of the high-energy band may be a result of two overlapping bands. It is noted that complexes **A** and **B** (Chart 1) each had three CN stretches (near 2157, 2080, and 2040 $cm^{-1}$); data for **C** were not reported.[6] Finally, the possibility that the solution dynamic process involves dissociation of one $CN^tBu$ is disfavored, owing to the negative value for activation entropy. Furthermore, the NMR resonances for free $CN^tBu$ or for (PNN)Rh($CN^tBu$) (***IA***) were not observed. As also noted in the Supporting Information, we have spectroscopically characterized ***IA*** as a synthetic intermediate along the way to **3**. The spectroscopic signatures of ***IA*** and its mixtures with **3** are different from the variable-temperature NMR spectral data.[11]

The structural adaptability of the new PNN-pincer type ligand is displayed by rhodium(III) complexes derived from **3**. Thus, as per Scheme 3, the reaction between **3** and MeI produced easily separable mixtures of *cis,mer* (hereafter referred to simply as *mer*, since the *trans,mer* isomer has not yet been detected) and *fac* isomers of [(PNN)Rh(Me)($CN^tBu)_2$](I), **4**. The *mer* isomer has some solubility in benzene, in contrast to the *fac* isomer, thereby allowing separation. Figures 3 and 4

**Scheme 3. Reaction between MeI and 3 in $CH_2Cl_2$**

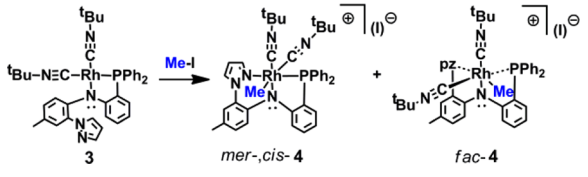


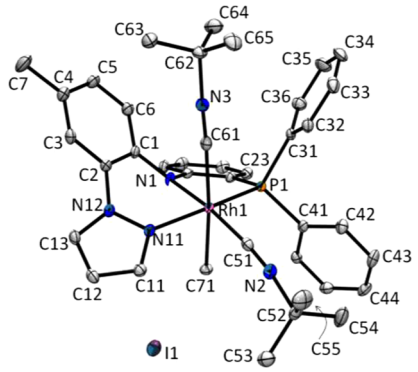


**Figure 3.** Structure of *cis,mer*-[(PNN)Rh(Me)($CN^tBu)_2$](I)·$C_6H_6$, (*mer*-**4**·$C_6H_6$). Selected bond distances (Å): Rh1−P1, 2.2420(6); Rh1−N1, 2.0684(18); Rh1−N11, 2.0969(19); Rh1−C51, 1.949(2); Rh1−C61, 2.074(2); Rh1−C71, 2.101(2); N2−C51, 1.151(3); N2−C52, 1.466(3); N3−C61, 1.146(3); N3−C62, 1.470(3); Selected bond angles (deg): P1−Rh1−N11, 166.78(5); N1−Rh1−C51, 175.30(9); C61−Rh1−C71, 175.08(9); P1−Rh1−C61, 95.51(6); C71−Rh1−N11, 85.21(8); N1−Rh1−C71, 86.48(9); N11−Rh1−N1, 85.34(7); P1−Rh1−N1, 82.67(6); C51−Rh1−C71, 88.86(9); C51−Rh1−C61, 93.40(9); C61−Rh1−N1, 91.20(8). Hydrogen atoms and benzene molecule have been omitted for clarity.

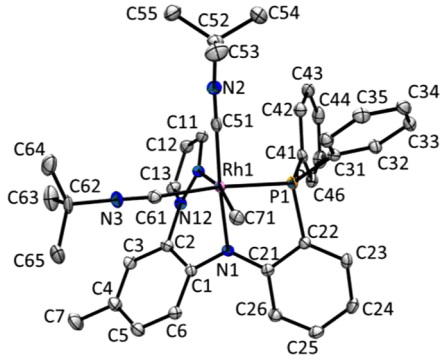


**Figure 4.** Structure of the cation in *fac*-[(PNN)Rh(Me)($CN^tBu)_2$]-(I)·$H_2O$ (*fac*-**4**·$H_2O$). Selected bond distances (Å): Rh1−P1, 2.2765(6); Rh1−N1, 2.0577(19); Rh1−N11, 2.176(2); Rh1−C51, 1.955(2); Rh1−C61, 2.040(2); Rh1−C71, 2.107(2); N2−C51 1.147(3); N2−C52 1.473(3); N3−C61 1.145(3); N3−C62 1.466(3). Selected bond angles (deg): N1−Rh1−C51, 175.79(9); P1−Rh1−C61, 174.33(7); C71−Rh1−N11, 167.91(8); P1−Rh1−N11, 96.46(5); N1−Rh1−C71, 87.62(9); N11−Rh1−N1, 81.98(7); P1−Rh1−N1, 81.01(6); C51−Rh1−C71, 89.96(10); C51−Rh1−C61, 88.92(9); C61−Rh1−N1, 94.46(9). Hydrogen atoms, the iodide anion, and the water molecule have been omitted for clarity.

show the structures of the cations in *mer*-**4** and *fac*-**4**, respectively. In these structures, the Rh−N1 distance of 2.068(2) Å (*mer*-**4**) and 2.058(2) Å (*fac*-**4**) are among the longest such bonds found in related (pincer)$Rh^{III}$ derivatives,[17] rivaling 2.064(2) Å in *trans*-(NNN)$RhCl_2(PEt_3)$. In fact, the Rh1−N1 distance in *mer*-**4** with a formal rhodium(III) center is close to the 2.0728(14) Å found in **3**, with a rhodium(I) center. For both *fac*- and *mer*-**4**, the $CN^tBu$ *trans* to the amido group has shorter Rh1−C51 and longer C51−N2 bonds versus the analogous bonds in the other $CN^tBu$ group (*trans* to the phosphine). This observation may be indicative of the greater $\pi$-donating abilities of the diarylamido versus the triarylphosphine group that increases the metal back-bonding to the *trans*-$CN^tBu$ ligand. This effect is also apparent in **3**. It is also worth noting that the Rh−$N_{pz}$ bond in *fac*-**4** is longer than that in *mer*-


dx.doi.org/10.1021/om400151e | *Organometallics* 2013, 32, 2885−2888

**4** or **3**, which might be related to the constrained ligand geometry in this coordination mode and the donating abilities of the ligand *trans* to the pyrazolyl nitrogen.

Interestingly, the ratio of *fac*- to *mer*-**4** obtained from the preparative reactions depends on the solvent and time allotted for reaction, as indicated by NMR spectroscopy (and X-ray crystallography). When the reaction was performed in dichloromethane, a 3:1 *fac*:*mer* ratio was immediately obtained. That is, upon addition of MeI to a $CD_2Cl_2$ solution of **3**, the original $^{31}P$ NMR doublet resonance at $\delta_P$ 46.0 ppm ($J_{P-Rh}$ = 141 Hz) was immediately replaced by two new doublet resonances at $\delta_P$ 57.8 ppm ($J_{P-Rh}$ = 121 Hz) and $\delta_P$ 54.3 ppm ($J_{P-Rh}$ = 106 Hz) in a 3:1 ratio. The former resonance with the larger coupling constant is due to *mer*-**4**, while the latter resonance with the smaller coupling constant is due to *fac*-**4**. Over time, the resonance for the *mer* isomer grows at the expense of that for the *fac* isomer. When the reaction between **3** and MeI was performed in a limited amount of benzene, pure *fac*-**4** (59%) immediately precipitated as a yellow solid; the soluble portion contained dark orange *mer*-**4** (40%). The reversal in isomer ratio in $C_6D_6$ in comparison to the reaction performed in $CD_2Cl_2$ is kinetic in nature. After the benzene-insoluble product (pure *fac*-**4**) was dissolved in $CD_2Cl_2$, the $^{31}P$ NMR spectrum showed complete conversion to *mer*-**4** over the course of 44 h with first-order kinetics ($t_{1/2}$ = 7.2 h; Figures S7, S8 (Supporting Information)). It is noteworthy that theoretical calculations indicate that the *mer* isomer is more stable than the *fac* isomer by about 2 kcal/mol (Table S10 (Supporting Information)).

In summary, a new easily crystallizable pincer-type ligand with a PNN donor set has been prepared. The $\kappa^2P,N$ coordination mode in its bis(organoisocyanide)rhodium(I) complex was structurally verified, a mode suggested by the van der Vlugt group for similar complexes. Hemilabile behavior of the pyrazolyl arm of the ligand to give four- and five-coordinate metal centers in $(PNN)Rh(CN^tBu)_2$ is suggested to be responsible for the dynamic solution behavior detected by NMR spectroscopy. The new PNN ligand was also found to exhibit both *fac* and *mer* coordination modes in its rhodium(III) complexes. The *mer* coordination mode is more stable than the *fac* mode, likely due to the lesser chelate ring strain and greater resonance stabilization associated with the increased planarity of the electroactive diarylamido moiety. The results of DFT calculations suggest that the *fac* mode and five-coordinate $(L)Rh(CN^tBu)_2$ complexes are not unique to the new PNN ligand (Figure S10 (Supporting Information)). However, the *fac*- mode is favored for the new ligand over that in related PNN ligands. Perhaps the semirigidity of the new PNN ligand with its finite dihedral angle between mean planes of pyrazolyl and aryl rings helps to minimize the energetic penalties associated with the ligand adopting the *fac* mode (i.e., there is better preorganization in the new ligand versus others). In this manner, the coordination behavior of the new ligand falls somewhere between that of a pincer and a heteroscorpionate. Future investigations will be directed at further examining the stoichiometric reactions and catalytic activity of rhodium(I) and other first-row transition-metal complexes of variants of this new PNN ligand.

## ■ ASSOCIATED CONTENT

### Ⓢ Supporting Information

Text, figures, tables, and CIF files giving experimental and computational details, NMR spectra, further discussion, and crystallographic data. This material is available free of charge via the Internet at http://pubs.acs.org.

## ■ AUTHOR INFORMATION


### Corresponding Author

*E-mail for J.R.G.: james.gardinier@marquette.edu.


### Notes

The authors declare no competing financial interest.

## ■ ACKNOWLEDGMENTS

J.R.G. thanks the NSF (CHE-0848515) for financial support.

## ■ REFERENCES


(1) (a) Zhanga, W.-H.; Chiena, S. W.; Hor, T. S. *Coord. Chem. Rev.* **2011**, *255*, 1991−2024. (b) Braunstein, P.; Naud, F. *Angew. Chem., Int. Ed.* **2001**, *40*, 680−699. (c) Slone, C. S.; Weinberger, D. A.; Mirkin, C. A. *Prog. Inorg. Chem.* **1999**, *48*, 233−350.

(2) (a) Grützmacher, H. *Angew. Chem., Int. Ed.* **2008**, *47*, 1814−1818. (b) Angell, S. E.; Rogers, C. W.; Zhang, Y.; Wolf, M. O.; Jones, W. E., Jr. *Coord. Chem. Rev.* **2006**, *250*, 1829−1841.

(3) Recent examples: (a) Jiménez, M. V.; Bartolomé, M. I.; Pérez-Torrente, J. J.; Gómez, D.; Modrego, F. J.; Oro, L. A. *ChemCatChem* **2013**, *5*, 263−276. (b) Tornatzky, J.; Kannenberg, A.; Blechert, S. *Dalton Trans.* **2012**, *41*, 8215−8225. (c) Hounjet, L. J.; McDonald, R.; Ferguson, M. J.; Cowie, M. *Inorg. Chem.* **2011**, *50*, 5361−5378.

(4) (a) Frauhiger, B. E.; White, P. S.; Templeton, J. L. *Organometallics* **2012**, *31*, 225−237. (b) Tsoureas, N.; Kuo, Y.-Y.; Haddow, M. F.; Owen, G. R. *Chem. Commun.* **2011**, *47*, 484−486. (c) Tsoureas, N.; Owen, G. R.; Hamilton, A.; Orpen, A. G. *Dalton Trans.* **2008**, 6039−6044.

(5) (a) Ruddy, A. J.; Mitton, S. J.; McDonald, R.; Turculet, L. *Chem. Commun.* **2012**, *48*, 1159−1161. (b) Fulmer, G. R.; Kaminsky, W.; Kemp, R. A.; Goldberg, K. I. *Organometallics* **2011**, *30*, 1627−1636. (c) Niu, J.-L.; Hao, X.-Q.; Gong, J.-F.; Song, M.-P. *Dalton Trans.* **2011**, *40*, 5135−5150. (d) van der Vlugt, J. I.; Pidko, E. A.; Vogt, D.; Lutz, M.; Spek, A. L. *Inorg. Chem.* **2009**, *48*, 7513−7515. (e) Zhang, J.; Leitus, G.; Ben-David, Y.; Milstein, D. *J. Am. Chem. Soc.* **2005**, *127*, 10840−10841.

(6) Lindner, R.; van den Bosch, B.; Lutz, M.; Reek, J. N. H.; van der Vlugt, J. I. *Organometallics* **2011**, *30*, 499−510.

(7) See for example: (a) Gloaguen, Y.; Jacobs, W.; de Bruin, B.; Lutz, M.; van der Vlugt, J. I. *Inorg. Chem.* **2013**, *52*, 1682−1684. (b) Wanniarachchi, S.; Liddle, B. J.; Toussaint, J.; Lindeman, S. V.; Bennett, B.; Gardinier, J. R. *Dalton Trans.* **2011**, *40*, 8776−8787. (c) Calimano, E.; Tilley, T. D. *Dalton Trans.* **2010**, *39*, 9250−9263.

(8) Liddle, B. J.; Silva, R. M.; Morin, T. J.; Macedo, F. P.; Shukla, R.; Lindeman, S. V.; Gardinier, J. R. *J. Org. Chem.* **2007**, *72*, 5637−5646.

(9) Winter, A. M.; Eichele, K.; Mack, H.-G.; Potuznik, S.; Mayer, H. A.; Kaska, W. C. *J. Organomet. Chem.* **2003**, *682*, 149−154.

(10) Wanniarachchi, S.; Liddle, B. J.; Lindeman, S. V.; Gardinier, J. R. *J. Organomet. Chem.* **2011**, *696*, 3623−3636.

(11) See the Supporting Information.

(12) Northcutt, T. O.; Lachicotte, R. J.; Jones, W. D. *Organometallics* **1998**, *17*, 5148−5152.

(13) Carlton, L.; Mokoena, L. V.; Fernandes, M. A. *Inorg. Chem.* **2008**, *47*, 8696−8703.

(14) Tejel, C.; Ciriano, M. A.; Edwards, A. J.; Lahoz, F. J.; Oro, L. A. *Organometallics* **1997**, *16*, 45−53.

(15) Jeffery, J. C.; Lebedev, V. N.; Stone, F. G. A. *Inorg. Chem.* **1996**, *35*, 2967−2976.

(16) Rubio, M.; Suárez, A.; del Río, D.; Galindo, A.; Álvarez, E.; Pizzano, A. *Organometallics* **2009**, *28*, 547−560.

(17) Wanniarachchi, S.; Liddle, B. J.; Kizer, B.; Hewage, J. S.; Bennett, B.; Lindeman, S. V.; Gardinier, J. R. *Inorg. Chem.* **2012**, *51*, 10572−10580.